Desalination and Water Treatment
www.deswater.com
doi: 10.1080/19443994.2015.1021840

57 (2016) 8228–8235
April

Numerical simulation of optimal submergence depth of impellers in an oxidation ditch

Wenli Wei*, Yuling Liu, Bin Lv

State Key Laboratory Base of Eco-Hydraulic Engineering in Arid Area, Xi'an University of Technology, Xi'an, Shaanxi 710048, China, Tel. +86 15596886263; email: wei_wenli@126.com (W. Wei), Tel. +86 18591999882; email: liuyuling@xaut.edu.cn (Y. Liu), Tel. +86 13991987708; email: lvbin_1@126.com (B. Lv)

Received 28 March 2014; Accepted 11 February 2015

ABSTRACT

Submergence depth of impellers for an oxidation ditch (OD) has significant impact on energy consumption and effluent quality of wastewater treatment plants. The effect of the submergence depth of impellers on the structure of flow fields in an OD was studied using an experimentally validated numerical tool, based on computational fluid dynamics (CFD) model. The two-phase gas–liquid model and the 3D RNG k–ε turbulence model were used to describe flow in ODs. The pressure implicit with splitting of operators algorithm was used to solve velocity and pressure. The volume of fluid (VOF) method was used to simulate free-water surface. The concept of submergence depth ratio representing the impeller's submergence depth h to the total water depth H, h/H, was introduced to analyze the simulation results. Under different submergence depth ratios of impellers in an OD, the velocity fields were computed and analyzed, which shows that with the submergence depth ratio 0.45, the percentage of VOF particles with velocity greater than 0.3 m/s to the volume of entire fluid particles is the greatest, and that the velocity distribution is more uniform along water depth, being much useful for preventing sludge from settling in ODs. Therefore, the submergence depth ratio 0.45 is called the optimal submergence ratio, and its corresponding operating condition will better improve the efficiency of an OD wastewater treatment system.

Keywords: Oxidation ditch; Numerical simulation; Optimal submergence depth; Flow field

1. Introduction

Oxidation ditches (ODs) have been widely used as an activated sludge biological treatment process, due to its reliability, simplicity of operation, and low-sludge production [1]. The optimal operation of an OD system is still challenging for wastewater treatment plants (WWTPs) because of economic and technical factors. Therefore, upgrading of existing OD systems to reduce operation costs is warranted for WWTPs. Since the OD process efficiency depends heavily on the flow field, the hydrodynamics of an OD has been studied for a successful design by physical tests and numerical simulation.

Xu et al. [2] adopted the CFD method and the particle image velocimetry (PIV) to investigate hydrodynamic characteristics in a Carrousel OD, and found that because of the effects of lateral slope of water surface and circulation flow in the curved region, low

*Corresponding author.

speed and/or stagnancy would occur easily in the inner part of the curved region, resulting in sludge sedimentation. Liu and He [3] used an acoustic Doppler velocimeter (ADV) to analyze the flow fields of ODs with submerged impellers, which indicated that when the submerged impeller was installed in the center of the cross section, the cross-sectional mean velocity was 18% higher than that installed at the bottom, and the power utility rate was also higher. Fan et al. [4] measured the flow field with a particle dynamic analyzer (PDA) in an experimental Carrousel OD with two surface aerators like inverse umbrellas. The distributions of the flow velocity, settling velocity, and solid volume fraction were obtained and analyzed in detail. Vermande et al. [5] have measured local gas retention, gas velocity, and bubble size, and linked to the classical global measurements of oxygen transfer coefficient and of horizontal liquid velocity; and have tested different operating conditions to show the impact of each parameter on hydraulics and aeration performance, which shows that an augmentation of the horizontal liquid velocity results in higher values for the global oxygen transfer coefficient, being confirmed by observation and local measurements. Xu et al. [6] studied the technique of PIV for liquid–solid two-phase flow field on the basis of the single-phase PIV investigation. The software was applied to investigate two-dimensional liquid–solid two-phase flow velocity of straight and flexural channels of a Carrousel OD. The disadvantages of the traditional measurement of getting velocities only at single point and of being unable to acquire the synchronic information of whole-flow-field were overcome. Fan et al. [7] simulated the turbulent solid–liquid two-phase flow field in the OD aerated with surface aerators like inverse umbrellas with CFD, and performed experiments in a laboratory-scale OD with a PDA, by which they found that the liquid and solid phases have similar flow velocity, while the vertical velocity of solid phase is slightly lower than that of liquid. Wei et al. [8] measured the velocity field in an OD model using ADV, by which the distribution profiles of both vertical and lateral velocities along the straight section were obtained, and the velocity patterns in the outer part were quite different from those in the inner part of the OD channels. Guo et al. [9] monitored the flow velocity and dissolved oxygen (DO) concentration in the outer channel of an Orbal OD system in a WWPT in Beijing under actual operation conditions, and simulated the flow field and DO concentration distributions by CFD. The monitoring and simulation showed that the flow velocity was heterogeneous in the outer channel; thus, the DO was also heterogeneously distributed in the outer channel with concentration gradients occurring along the flow direction as well as in the cross section. This heterogeneous DO distribution created many anoxic and aerobic zones, which may have facilitated simultaneous nitrification–denitrification in the channel. These findings may provide support for rational optimization of the performance of the Orbal OD.

However, with the development of computer technology, CFD has been used more commonly in wastewater treatment recently. Liu et al. [10] studied the effect of the size of impeller's radius on the structure of flow fields in an OD using the two-phase gas–liquid model, and obtained the optimal radius' ratio 0.218 of impellers. Li et al. [11] used Fluent software to simulate the flow field in an OD. The moving wall model was used to simulate impellers in the ditch. The simulation of flow in the deeper OD, with and without installing guide baffle, shows that installing parameters of guide baffle has a great influence on flow field, and proper installing parameters of guide baffle can efficiently improve velocity distribution, and reduce the possibility of sludge sedimentation. Xing and Qiu [12] proposed a new kind of impeller with curve blades, and the flow field driven by the new impellers in an OD was simulated with the ANSYS software, which provides a reference data for optimization design of the mixing blades. Fayolle et al. [13] proposed an experimentally validated numerical tool to predict flow and oxygen transfer characteristics in aeration tanks equipped with fine bubble diffusers and axial slow speed mixers. Predicted oxygen transfer coefficients are within ±5% of experimental results for different operating conditions. Wang et al. [14] did some simulation and improvement for the bend flow field of an OD. The simulation results show that the straight diversion wall of an OD should be as long as the straight channel, the arrangement of the two guide walls in the bends can weaken the transverse circulation and eliminate the low velocity zone near concave walls, preventing the sludge from settling. Zhang et al. [15] simulated the flow characteristics of an anoxic zone of an OD in Chongqing Jingkou WWTP by CFD, according to which the proper setting location of a submerged impeller and the suitable setting way of a training wall were proposed, by which under the same power density, the flow is more uniform, effectively preventing or reducing the ditch sludge deposition. Xie et al. [16] proposed a two-phase (liquid–solid) CFD model for simulating the flow field and sludge settling in a full-scale OD, in which the Takács double-exponential sedimentation velocity function was used. Based on the simulation results of the flow field and sludge settling, an optimized operation scheme of the OD was proposed. Compared with the existing one, the volume fraction of solid phase at the bottom of the OD in the optimized operation scheme was decreased, making the distribution of sludge more uniform. Tang et al. [17] established a 3D submerged impeller model, combining with a multiple reference frame (MRF) model and RNG k–ε turbulence model, to simulate the flow fields in an OD. The characteristics of the flow field in the OD were successfully and effectively simulated.

Operating conditions of submerged impellers for an OD have significant impact on energy consumption and effluent quality of WWTPs. Flow motion in an OD results from the moving impellers, and the flow field structure is closely related to the factors of the impellers, such as submergence depth, radius, and running speed, etc. *The above research does not relate to the optimization of impellers' submergence depth.* Therefore, this paper studies the relation between the impellers' submergence depth and the flow field structure with the same radius and running speed in an OD using a numerical simulation method to find the optimal submergence depth of impellers.

2. Definition of non-uniform velocity coefficient

In order to quantitatively analyze the uniformity of flow velocity distribution, the non-uniform velocity coefficient was introduced, and is defined as the ratio of the difference between maximum and minimum velocity to the average velocity along the vertical direction on the cross section, the formula for which is:

$$\eta = (V_{\max} - V_{\min}) \ / \ V_{\text{ave}} \tag{1}$$

where η is the non-uniform velocity coefficient, $V_{\max}$ and $V_{\min}$ are the maximum and minimum flow velocities along the vertical direction on the cross section, respectively, and V_{ave} is the average flow velocity of the cross section.

According to the definition of non-uniform velocity coefficient, it is known that the larger the non-uniform velocity coefficient, the more non-uniform is the velocity distribution.

3. Definition of optimal submergence depth ratio

The relation between the submergence depth of impellers and the structure of flow field in an OD with the same impeller's radius and running speed was studied. The OD designing rule requires the fluid cross-sectional average velocity to be greater than 0.3 m/s; thus, the percentage of volume of fluid particles with velocity greater than 0.3 m/s to the volume of total fluid particles, P, is taken as a variable, and the ratio of an impeller submergence depth to the total water depth, h/H, as another dimensionless parameter, and draw a curve of P varying with h/H under the same impeller's radius and running speed. When P gets to the greatest, its corresponding h/H is called the optimal submergence depth ratio of impellers.

4. Mathematical model

4.1. Governing equations

The 3D Reynolds-averaged Navier–Stokes equations governing unsteady, compressible flow for continuity, and momentum can be written as [18]:

Continuity equation:

$$\frac{\partial \rho}{\partial t} + \frac{\partial(\rho u_i)}{\partial x_i} = 0 \tag{2}$$

Momentum equation:

$$\frac{\partial(\rho u_i)}{\partial t} + \frac{\partial(\rho u_i u_j)}{\partial x_j} = -\frac{\partial p}{\partial x_i} + \frac{\partial}{\partial x_j}\left[\mu\left(\frac{\partial u_i}{\partial x_j} + \frac{\partial u_j}{\partial x_i}\right)\right] - \frac{\partial}{\partial x_j}\left(\rho\overline{u'_i u'_j}\right) + \rho g_i \tag{3}$$

where ρ is the density (in water, ρ is equal to the water density; in air, ρ is equal to the air density), t is the time, x_i is the space coordinate in i direction, p is the pressure, μ is the molecular kinematic viscosity, g_i is the gravitational acceleration in i direction, u_i is the velocity component in i direction, u'_i is the fluctuating velocity component in i direction, and the subscripts i, $j = 1, 2, 3$.

The turbulence stress term $-\rho\overline{u'_i u'_j}$ is computed from [19]:

$$-\rho\overline{u'_i u'_j} = \mu_t\left(\frac{\partial u_i}{\partial x_j} + \frac{\partial u_j}{\partial x_i}\right) - \frac{2}{3}\left(\rho k + \mu_t \frac{\partial u_i}{\partial x_i}\right)\delta_{ij} \tag{4}$$

where δ_{ij} is the Kronecker function, and μ_t is the kinematic viscosity, being determined by the following formulas [18,19]:

$$\mu_t = \rho C_\mu \frac{k^2}{\varepsilon} \tag{5}$$

where k is turbulent kinetic energy, ε is kinetic energy dissipation rate, and C_μ is a constant.

The estimation of μ_t utilizes the RNG k–ε turbulence model, the equations of which are given by Liu et al. [18].

Turbulent kinetic energy k equation:

$$\frac{\partial(\rho k)}{\partial t}+\frac{\partial(\rho k u_{\mathrm{i}})}{\partial x_i}=\frac{\partial}{\partial x_j}\left[\left(\mu+\frac{\mu_t}{\sigma_k}\right)\frac{\partial k}{\partial x_j}\right]+G_k-\rho\varepsilon \tag{6}$$

Kinetic energy dissipation rate ε equation:

$$\frac{\partial(\rho\varepsilon)}{\partial t}+\frac{\partial(\rho\varepsilon u_i)}{\partial x_i}=\frac{\partial}{\partial x_j}\left[\left(\mu+\frac{\mu_t}{\sigma_\varepsilon}\right)\frac{\partial\varepsilon}{\partial x_j}\right]+C_1\frac{\varepsilon}{k}G_k-\rho C_2\frac{\varepsilon^2}{k} \tag{7}$$

where C_μ, σ_k, C_2, and σ_ε are empirical constants and have the value of 0.085, 0.7179, 1.68, and 0.7179, respectively, and other parameters are: $C_1=1.42-\frac{\tilde{\eta}(1-\tilde{\eta}/\tilde{\eta}_0)}{1+\beta\tilde{\eta}^3}$, $\tilde{\eta}=\mathrm{Sk}\backslash\varepsilon$, $S=(2S_{i,j}S_{i,j})^{1/2}$, $\tilde{\eta}_0=4.38$ $\beta=0.015$, $S_{i,j}=\frac{1}{2}\left(\frac{\partial u_{\mathrm{i}}}{\partial x_j}+\frac{\partial u_j}{\partial x_i}\right)$.

4.2. VOF method

To describe the liquid–gas interface, the VOF method [19] is used. The volume of water inside a cell is computed from $V_{\mathrm{w}} = F \times V_{\mathrm{c}}$, where V_{c} is the volume of the cell, and F is the liquid volume fraction in a cell, being defined as the ratio of cell volume occupied by liquid to total volume of the control cell. The value of F in a cell ranges from 0 to 1. Here, $F = 1$ represents a cell completely filled with liquid, $F = 0$ represents a cell completely filled with gas, and $0 < F < 1$ represents the liquid–gas interface. The liquid volume fraction distribution can be determined by solving a separate passive transport equation, given as:

$$\frac{\partial F}{\partial t}+\frac{\partial(F u_{\mathrm{i}})}{\partial x_{\mathrm{i}}}=0 \tag{8}$$

The physical properties of mixture are derived from those of water and air by the volume fraction function. In particular, the average values of ρ and μ in a computational cell can be computed from the value of F in accordance with:

$$\rho=(1-F)\rho_{\mathrm{a}}+F\rho_{\mathrm{w}} \tag{9}$$

$$\mu=(1-F)\mu_{\mathrm{a}}+F\mu_{\mathrm{w}} \tag{10}$$

where ρ_a and μ_{a} are the density and viscosity of air, respectively, and ρ_{w} and v_{w} are the density and viscosity of water, respectively.

4.3. Initial and boundary conditions and solution method

It was found that the inlet and outlet flow conditions for an OD have little influence on the flow field, so they were ignored in the numerical calculation. Boundary condition at the top surface of the computational domain was given as a relative pressure zero, and that at the side walls and the bottom was given by the wall function. The motion of submerged impellers relative to the OD was described by a MRF model with sliding mesh method. The initial condition was given as a stationary water depth. The rotation speed of submerged impellers was specified.

The RNG k–ε turbulent model was used to close the 3D Reynolds-averaged Navier–Stokes equations, the convection terms were discretized by first-order upwind scheme, and the PISO algorithm was used to solve velocity and pressure. The free surface was simulated according to the VOF method.

5. Result analysis and discussion

5.1. Calculated model

The side wall of the Carrousel OD to be studied is 5 m high, and about 115 m long, and the water depth is 4.5 m high. The capacity of the wastewater treatment is 25,000 m^3/D. Three impellers with a speed of 30 r/min are arranged at both ends of the OD, shown in Fig. 1(a). In the numerical calculation, the computational domain is 109 m long, 34.6 m wide, and 6 m high. As can be seen, the height of the computational domain is 1.5 m greater than its water depth; this is required for the simulation method of free-water surface with the VOF method. The OD consists of four channels, A, B, C, and D. Each channel is 8.5 m wide; the radius of the small bend is 8.5 m, and of the big bend is 17 m. The thickness of the Carrousel diversion wall is 0.2 m, as shown in Fig. 1(b).

5.2. Grid generation

Fig. 2(a) shows the 3D computational domain. Fig. 2(b) shows the 2D grid of plane of the computational domain. The 3D computational domain was divided into 30 layers. The total number of the elements of 3D grid is 2.5×10^5.

5.3. Statistical analysis of optimal submergence depth ratio

Here, the flow fields for five different submergence ratios of impellers of 0.10, 0.22, 0.45, 0.67, and 0.89 were computed. The designing rule requires the average cross-sectional velocity in an OD to be greater

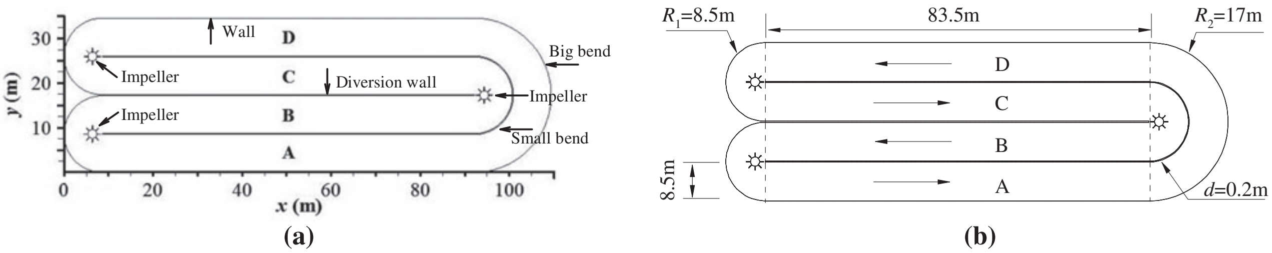

Fig. 1. 2D Horizontal plane of the computational domain (a) details of the structure and (b) details of the size of structure.

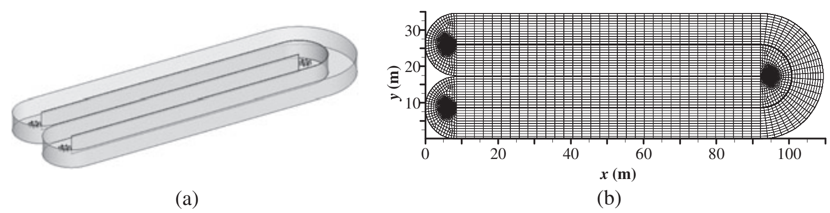

Fig. 2. Grid of the computational domain. (a) 3D computational domain and (b) 2D grid of plane of the computational domain.

than 0.3 m/s, according to which the optimal submergence depth of impellers is obtained. The percentage of the volume of fluid particles with a velocity greater than 0.3 m/s to the volume of total fluid particles, P, as a variable, and the ratio of the impeller's submergence depth to the total water depth, h/H, as another dimensionless parameter were taken, and the curve of P varying with h/H was drawn as shown in Fig. 3. P is dependent on h/H, which shows that with increasing h/H, P increases at first and then decreases; when P gets to the biggest value, h/H equals to 0.45. The submergence depth ratio $h/H = 0.45$ is called as the optimal submergence depth of impellers.

5.4. Analysis of velocity distribution along water depth

The submergence depth of impellers in an OD has an important influence on the velocity distribution along vertical direction. The OD by the simulation consists of four channels, A, B, C, and D. The velocity distribution along four vertical lines in channel A are chosen to analyze, and the four vertical lines are located at $x = 20$ m (Location 1), $x = 40$ m (Location 2), $x = 60$ m (Location 3), and $x = 80$ m (Location 4), as shown in Fig. 4.

The flow velocity distribution along water depth varies with the submergence depth of impellers. Under the two submergence depth ratios of $h/H = 0.22$ and 0.45, the computed velocity distributions along the four vertical lines at $x = 20$ m, $x = 40$ m, $x = 60$ m, and $x = 80$ m are plotted in Fig. 5, where v means velocity value, from which it was found that with the submergence depth ratio 0.45 comparing with 0.22, the flow velocity at upper region increases obviously, and at lower region decreases, which means that the flow along the water depth becomes more

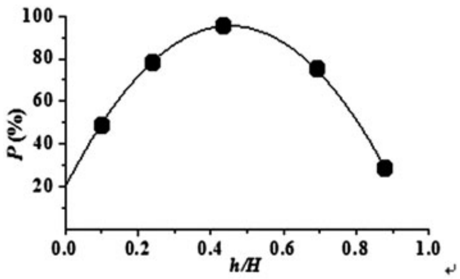

Fig. 3. Curve of P varying with h/H.

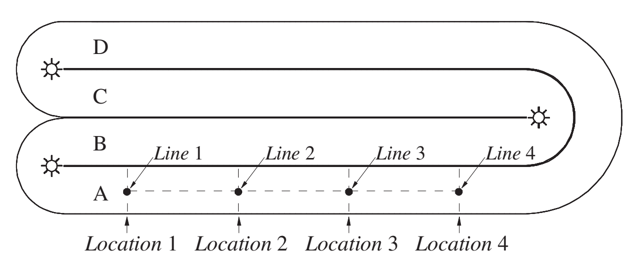

Fig. 4. Location of vertical lines.

uniform with the submergence depth ratio of 0.45 than with 0.22.

The flow velocity distribution was analyzed by the method of non-uniform velocity coefficients. The computational non-uniform velocity coefficients for the four vertical lines are shown in Table 1, from which it was found that for the same vertical line, the computed non-uniform velocity coefficient is smaller when the impellers are submerged at the ratio of 0.45 than at 0.22. In view of the definition of non-uniform velocity coefficient, it is known that the velocity distribution becomes more uniform when the impellers are submerged at the ratio of 0.45 rather than of 0.22.

By a similar method, it can also be obtained that the flow along water depth becomes more uniform with the submergence depth ratio of 0.45 than that of 0.10, 0.67, and 0.89, which is more useful for preventing sludge from settling in ODs. Therefore, the impellers with the optimal submergence ratio of 0.45 will better improve the efficiency of OD sewage treatment system.

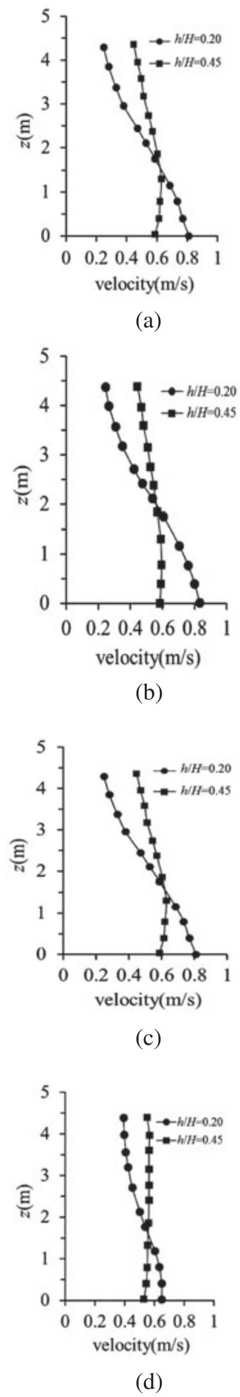

Fig. 5. Velocity distributions for the vertical lines. (a) at x = 20 m (Location 1), and (b) at x = 40 m (Location 2), (c) at x = 60 m (Location 3), and (d) at x = 80 m (Location 4).

5.5. Analysis of velocity distribution on a horizontal plane

The velocity vectors and velocity image at the horizontal plane located at 2.0 m depth from the water surface (2.5 m from the bottom) are shown in Fig. 6(a) and (b), respectively. When a moving vane makes a fluid move, and changes its momentum, forces are exerted between the vane and the fluid and work is done by displacement of the vane. The vane, by continuously doing work on the fluid, adds to its energy. The fluid continuously extracts energy from the vanes, and converts it into kinetic energy. The farther the position on the vane in contact with the fluid away from the rotating axis is, the larger is its displacement, and the more work is done, and vice versa; the farther the fluid in contact with the vane is away from the rotating axis is, the greater its kinetic energy is, and vice versa. Fluid particles collide with each other, thus the momentum is transmitted to each other; the momentum produced by the vanes is the dominant force (relative to the momentum of the influent flow), dictating the movement of the flow near the vanes. According to the velocity profiles, the zones near impellers are directly influenced by the mixing

Table 1
Computed non-uniform velocity coefficients

x	20 m		40 m		60 m		80 m	
h/H	0.20	0.45	0.20	0.45	0.20	0.45	0.20	0.45
V_{max}	0.76	0.65	0.83	0.594	80	0.628	0.65	0.57
V_{min}	0.29	0.48	0.23	0.44	248	0.446	0.39	0.55
V_{ave}	0.57	0.58	0.53	0.54	53	0.554	0.51	0.56
η	0.82	0.28	1.13	0.29	1.04	0.33	0.50	0.03

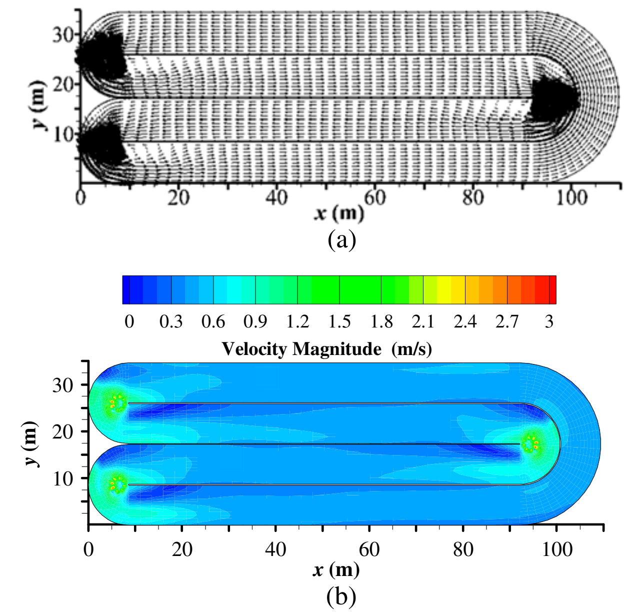

Fig. 6. Computed velocity vectors and magnitude at a horizontal plane located at 2.0 m depth from the water surface. (a) velocity vectors and (b) velocity magnitude.

induced by the impellers, shown in Fig. 6(a) and (b). Because of the centrifugal inertia force exerted on the flow in the bends, the non-uniformity of flow at the outlets of the bends is strengthened: near the inner walls, the velocity is smaller; and near the outer walls, the velocity is greater; which makes circulations appear near the outlets of the bends in straight sections; while in other parts of the straight regions, the flow is nearly uniform, as shown in Fig. 6(a).

6. Some discussion and further study plan

Numerical simulation and experimental study method are dependent upon each other. Experiment is the main way to investigate a new basic phenomenon, taking a large amount of observation data as the foundation; still, whether the numerical simulation result is correct or not must use the measured (prototype or model) data for validation. Doing numerical simulation in advance can obtain the preliminary results which can make the corresponding experiment plan more purposeful, and often reduce the number of tests needed by systematically doing experiments, and are much useful for the design of experimental device.

Here an experimentally validated numerical tool was used to study the effect of the submergence depth of impellers on the structure of flow fields in an OD, and obtained the optimal submergence depth ratio 0.45. Next, further study will be done to validate the simulation model by experimental method. An experiment with a 1:50 scale model made of organic glass for the Carrousel OD will be performed according to the gravity similarity theory. ADV will be used to measure velocities of the test model for the OD with different submergence depth ratios 0.10, 0.22, 0.45, 0.67, and 0.89 of propellers. The three points for measuring the velocities are, respectively, arranged at 0.2, 0.4, and 0.8 of the water depth from the ditch bottom, along the four given vertical lines corresponding to those in the prototype shown in Fig. 4. The gravity similarity theory (also named Froude number similarity theory) states that the relationship between the velocity values in the prototype and model is $\lambda_v = v_P/v_M = \lambda_L^{0.5}$, where the subscripts p and m denote prototype and model, and λ_v and λ_L ($\lambda_L = 50$) are velocity and length scale ratios, respectively. After measuring the velocity values, the corresponding values can be computed in the prototype. Finally, the measured velocity values will be compared with calculated data, which will further verify the reliability of the calculation.

7. Conclusion

The proposed numerical simulation method can be used to compute the flow fields of an OD to obtain optimal submergence ratio of impellers. With the optimal impellers' submergence depth ratio 0.45, the volume of fluid particles with a velocity greater than 0.3 m/s is greater than that with any other impellers' submergence depth ratios, and the velocity distribution along the vertical direction is more uniform than that with any other impellers' submergence depth ratios, which is useful for preventing sludge from settling. Thus, the flow with the optimal impellers' submergence depth ratio 0.45 will better improve the efficiency of sewage treatment of an OD system.

Acknowledgments

Financial support of this study was from the National Natural Science Foundation of China (Grant No. 51178391), the Scientific Research Project of Shaanxi Province (2014K15-03-05), and special funds for the development of characteristic key disciplines in the local university supported by the Central Financial fund (Grant No. 106-00X101, 106-5X1205) were greatly appreciated.

References

[1] Y. Yang, J.-K. Yang, J.-L. Zuo, Y. Li, S. He, X. Yang, K. Zhang, Study on two operating conditions of a full-scale oxidation ditch for optimization of energy consumption and effluent quality by using CFD model, Water Res. 45 (2011) 3439–3452.

[2] D.-Y. Xu, D.-J. Zhang, H.-N. Ai, Z. Chen, S.-F. Yang, Numerical simulation and experimental study of hydrodynamic characteristic in the Carrousel oxidation ditch reactor, Chin. J. Environ. Eng. 1(12) (2007) 20–26.

[3] Q.-l. Liu, J.-j. He, Submerged propeller's influence on oxidation ditch flow characteristics, Environ. Sci. Technol. 35(11) (2012), 93–98+134.

[4] L. Fan, Z.-q. Wang, Y.-c. Liu, D.-f. Chen H.-c. Shi, Experimental study of the flow in a Carrousel oxidation ditch equipped with two aerators by PDA, J. Hefei Univ. Technol. 30(11) (2007) 1454–1457.

[5] S. Vermande, K. Simpson, K. Essemiani, C. Fonade, J. Meinhold, Impact of agitation and aeration on hydraulics and oxygen transfer in an aeration ditch: Local and global measurements, Chem. Eng. Sci. 62(9) (2007) 2545–2555.

[6] D.-y. Xu, D.-j. Zhang, Z. Chen, Y.-c. Guo, W. Dai, Research on the particle image velocimetry for two-phase flow and experiment analysis in Carrousel oxidation ditch reactor, Chin. J. Environ. Eng. 1(8) (2007) 78–85.

[7] L. Fan, N. Xu, Z.-q. Wang, H.-c. Shi, PDA experiments and CFD simulation of a lab-scale oxidation ditch with surface aerators, Chem. Eng. Res. Des. 88 (2010) 23–33.

[8] Y.-f. Wei, J.-j. He, Z.-j. Li, Q.-l. Liu, Hydraulic characteristics in straight section of oxidation ditch, Environ. Sci. Technol. 35(12) (2012) 87–91.

[9] X.-s. Guo, X. Zhou, Q.-w. Chen, J.-x. Liu, Flow field and dissolved oxygen distributions in the outer channel of the Orbal oxidation ditch by monitor and CFD simulation, J. Environ. Sci. 25(4) (2013) 645–651.

[10] Y.-L. Liu, W.-l Wei, B. Lü, Research on optimal radius ratio of impellers in an oxidation ditch by using numerical simulation, Desalin. Water Treat. 52 (2014) 2811–2816.

[11] L. Li, J.-j. He, Q. Feng, Numerical simulation of guide plate influence on flow field in the oxidation ditch, Environ. Sci. Technol. 37(2) (2014) 149–154.

[12] P. Xing, B.-B. Qiu, The oxidation ditch flow field analysis pushed by the new type surface inverted umbrella aerator, Mach. Design Manuf. 1 (2014) 53–55.

[13] Y. Fayolle, A. Cockx, S. Gillot, M. Roustan, A. Héduit, Oxygen transfer prediction in aeration tanks using CFD, Chem. Eng. Sci. 62 (2007) 7163–7171.

[14] H.-j. Wang, Y.-b. Guo, Y.-x. Hu, Numerical simulation of flow fields of oxidation ditch bends, Energy Environ. 6 (2009) 10–12.

[15] Z. Zhang, H. Chai, B.-l. Li, Simulation on three-dimensional flow field and improvement on structure of anoxic zone of A~2O oxidation ditch, Chin. J. Environ. Eng. 1 (2012) 46–50.

[16] H. Xie, J.-k. Yang, Y.-c. Hu, H. Zhang, Y. Yang, K. Zhang, X.-f. Zhu, Y. Li, C.-z. Yang, Simulation of flow field and sludge settling in a full-scale oxidation ditch by using a two-phase flow CFD model, Chem. Eng. Sci. 109 (2014) 296–305.

[17] Y.-q. Tang, J.-j. He, Q.-l. Liu, Numerical simulation of flow fields in an oxidation ditch of taking a submerged propeller as the power, Chin. J. Hydrodyn. 3 (2013) 317–323.

[18] Y.-l. Liu, B. Lü, W.-l. Wei, 3D numerical simulation of the influence of impeller's radius on the length of flow recirculation in an oxidation ditch, J. Northwest A&F Univ. (Nat. Sci. Ed.) 42(2) (2014) 229–234.

[19] W.-l. Wei, H.-c. Dai, Turbulence Model Theory and Engineering Applications, Shanxi Science and Technology Press, Xi'an, 2006.